

Evaluation of the Ozone Monitoring Instrument's pre-launch radiometric calibration using in-flight data

M.G.Kowalewski*^a, G.Jaross^a, R.P.Cebula^a, S.L.Taylor^a,
G.H.J.van den Oord^b, M.R.Dobber^b, R.Dirksen^{b,c}

^aScience Systems and Applications Inc., 10210 Greenbelt Road, Lanham, MD, USA 20706;

^bRoyal Netherlands Meteorological Institute, PO Box 201, 3730 AE De Bilt, The Netherlands;

^cSpace Research Organization Netherlands, Sorbonnelaan 2, 3584 CA Utrecht, The Netherlands

ABSTRACT

Launched on 15 July 2004 aboard the EOS AURA satellite, the Ozone Monitoring Instrument (OMI) is intended as the successor to the Total Ozone Mapping Spectrometer (TOMS). OMI's improved horizontal spatial resolution and extended wavelength range (264-504nm) will provide total column ozone, surface reflectance, aerosol index, and ultraviolet (UV) surface flux as well as ozone profiles and tropospheric column ozone, trace gases, and cloud fraction and height.

We present results from a variety of calibration techniques that have been developed over the years to assess the calibration accuracy of backscatter UV sensors. Among these are comparisons of OMI solar measurements with external solar reference spectra and radiances measured over Antarctica and Greenland. OMI UV measured irradiances show wavelength dependencies and spectral features on order of 5% when compared to external solar spectra while all channels exhibit a nearly wavelength independent 1% seasonal goniometric error. No instrument throughput degradation has been identified beyond this level and has been confirmed through ice radiance comparisons. A 3% OMI radiance cross-track swath dependence is seen when comparing radiances over ice fields to radiative transfer results. Radiance residuals from total column ozone retrievals show the same cross-track swath dependence with an additional 5% offset.

Keywords: OMI, AURA, ultraviolet, calibration, ozone, backscatter

1. INTRODUCTION

The Ozone Monitoring Instrument (OMI) was launched onboard the EOS AURA satellite on 15 July 2005. As a successor to the NASA Total Ozone Mapping Spectrometer (TOMS), OMI's purpose is to produce daily global measurements of total column ozone and continue the long-term global ozone data record generated by the TOMS series of instruments. Other traditional TOMS data products, such as aerosol index, surface reflectance, and UV surface reflectance, are also produced. Utilizing the high spatial and spectral resolutions of the OMI instrument, scientists are additionally able to determine ozone profiles, tropospheric column ozone, trace gas column amounts of NO₂, BrO, HCHO and OCIO, and cloud fraction and height. Science teams from both NASA and the Royal Netherlands Meteorological Institute (KNMI) can utilize these data to help answer questions regarding the recovery of the ozone layer, tropospheric air pollution, and climate change.

As one of the primary goals, continuing the TOMS ozone data record necessitates that an accurate instrument calibration be maintained throughout the planned five-year lifetime of the instrument. OMI retrievals make use of the backscattered radiation from the Earth's atmosphere normalized to the observed solar irradiance. Referred to as albedo, it is this calibration for which the absolute and wavelength dependent nature must be characterized. Additionally, OMI observed radiances may be used in conjunction with radiances and products from other flight instruments, thus requiring a precise knowledge of instrument performance.

Over the course of the TOMS instrument legacy, a set of calibration techniques utilizing in-flight measured radiances and irradiances have been developed. Jaross *et al* confirmed instrument throughput changes in TOMS/Meteor3 by using observations of Antarctic ice fields¹ and was later applied to TOMS/EP. This same technique was later used for the NOAA-11 SBUV/2 instrument as the primary method of tracking throughput changes after the solar diffuser mechanism failed². Additional methods of using in-flight data, such as using radiance residuals from column ozone retrievals³, have been used to further enhance and validate in-flight instrument calibrations.

The purpose of this paper is to provide an overview of some of the current OMI calibration issues through the application of in-flight calibration techniques. In section 2, we shall provide a description of the instrument and its calibration activities. Analysis results of in-flight data, including irradiance and radiance measurements, are presented in section 3, and summarized in section 4.

2. INSTRUMENT DESCRIPTION

As part of the NASA A-train of satellites, the Aura spacecraft was launched into a sun-synchronous orbit inclined at 98°, nominal altitude of 705km, and local equator crossing time of 1342. Coupling this orbit with a large 114° field of view (FOV) and 2600km cross-track swath, OMI provides continuous, daily global coverage.

The OMI instrument consists primarily of a wide-field telescope, the optical bench, and two back-thinned, silicon charge coupled devices (CCDs). The optical bench and CCD detectors are operated at approximately 265K and maintained to within +/-300mK and +/-10mK, respectively. OMI's spectral range is broken into separate channels, ultraviolet (UV) and visible (VIS), and split by a dichroic into the proper optical path. The UV channel is further split into two sub-channels, referred to as UV-1 and UV-2, in order to handle the large dynamic range of the input Earth radiance and to maximize stray light rejection. Table 1 shows the spectral ranges, resolutions, and sampling for each channel.

Table 1. OMI performance characteristics

Channel	Wavelength Range [nm]	Spectral Resolution [nm]	Spectral Sampling [nm/pxl]
UV-1	264-311	0.63	0.33
UV-2	307-383	0.42	0.14
VIS	350-504	0.63	0.21

Each CCD has 780 spectral columns and 576 spatial pixel rows. The electronics and instrument control unit, called the ELU, digitizes the measured signals and transfers the data and commands to and from the instrument. The ELU and detector system is capable of on-chip binning to reduce data flow and increase signal to noise. All channels are nominally operated in a mode where the spatial dimension is binned by a factor of 8, yielding a total of 60 spatial pixels for UV-2 and VIS. In order to increase signal to noise, the UV-1 channel is imaged onto the CCD in an area half the size of UV-2 in the spatial dimension, yielding 30 binned spatial pixels. This nominal binning produces a ground pixel size of 13x24km for UV-2 and VIS, and 13x48km for UV-1. Figure 1 shows the optical layout of the instrument.

Ground calibration was performed with the instrument under flight-like conditions. Absolute radiance and irradiance calibrations were performed as well as instrument albedo. In order to properly track on-orbit calibration and performance issues, the instrument has a quartz volume diffuser (QVD) and two secondary ground aluminum diffusers. Daily, solar irradiance measurements are made with the QVD to track instrument throughput changes while the two ground aluminum diffusers are used to track any changes in the QVD. These measurements are performed at the Northern Hemisphere terminator and last approximately two minutes. Data collected from between $\pm 3^\circ$ are processed and averaged in time to create a final solar irradiance spectrum. Lastly, a transmission diffuser is used to couple light from an internal white light source that provides additional information on instrument throughput changes and detector characteristics.

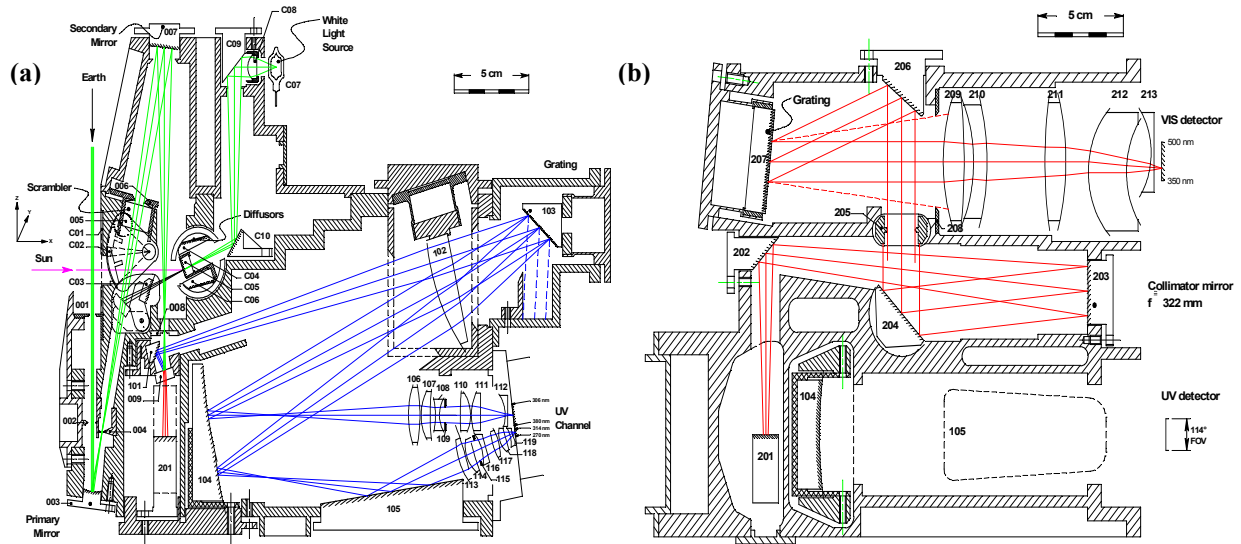


Figure 1. OMI optical path. The foreoptics and UV channels are shown in (a) as green and blue lines, respectively. The solar input direction is represented by the purple line in (a). The VIS channel is shown in (b) as red lines.

3. RESULTS

3.1. Solar irradiance observations

At wavelengths greater than 300nm, the Sun's stable spectral irradiance provides for an excellent on-orbit calibration source. Repeated solar observations performed by OMI provide a means to track the absolute irradiance calibration, instrument throughput changes, and swath angle dependence. All of these instrument characteristics directly affect the albedo calibration that is used to derive many of the OMI data products.

3.1.1. Absolute irradiance comparisons

The absolute irradiance calibration of OMI can be verified by comparing the measured solar irradiance to external references. At KNMI, an OMI solar reference spectrum has been developed that convolves the row and wavelength dependent OMI slit function with high-resolution solar spectra from literature. The ratio between an OMI solar irradiance measurement, taken during orbit 2465 on 31 December 2004, and the OMI solar reference spectrum is shown in Figure 2. This orbit is of particular interest as it is when the instrument azimuth angle equals the nominal azimuth used during ground calibration. Each channel, shown as a separate color, exhibits some interesting features. The both UV channels have a 7-8% wavelength dependence and a large discontinuity in their channel overlap regions. Residual Fraunhofer spectral structure can be seen in the lower wavelengths of UV-2 and a steep drop-off beyond 360nm is evident.

The wavelength dependence in UV-1 and UV-2 can possibly be attributed to issues in the ground calibration, such as stray light and source calibration. The high wavelength drop-off in UV-2 and turn-up in UV-1 may be the result of low signal-to-noise in both the solar irradiance measurements and the instrument irradiance calibration as these features lie closely to the edges of the channel response. Issues related to the solar reference spectrum, such as the convolution of the instrument spectral slit function with the high-resolution literature spectrum, and other residual instrument characterization errors, such as pixel response non-uniformity and spectral diffuser features, may be the cause of the residual Fraunhofer structure in UV-2.

The VIS channel comparison to reference yields a relatively flat spectral dependence. The process of combining high-resolution literature spectra from multiple sources may be the source of the spectral structure towards the lower end of the channel. Future work will include optimizing the solar reference spectrum as well as investigating the spectral dependence in the instrument irradiance calibration. However, the overall absolute irradiance calibration is shown to be relatively accurate and is comparable to other inter-instrument solar irradiance comparisons^{4,5}. For example, the MODIS/Aqua solar irradiances from reflective Bands 3, 8, 9, and 10 are plotted in Figure 2 relative to the OMI reference spectrum. Only a small 2% offset exists between the two instruments lending confidence in the accuracy of OMI's VIS channel solar irradiance calibration. Solar irradiances from the TOMS/EP instrument are also shown in Figure 2. A large, wavelength dependent offset is clearly seen, and suggests that OMI's UV-2 measured irradiances are approximately 8-10% too high. This is consistent with previous comparisons between TOMS/EP and SSBUV flight 7 irradiances where a similar offset and wavelength dependence was also seen⁶.

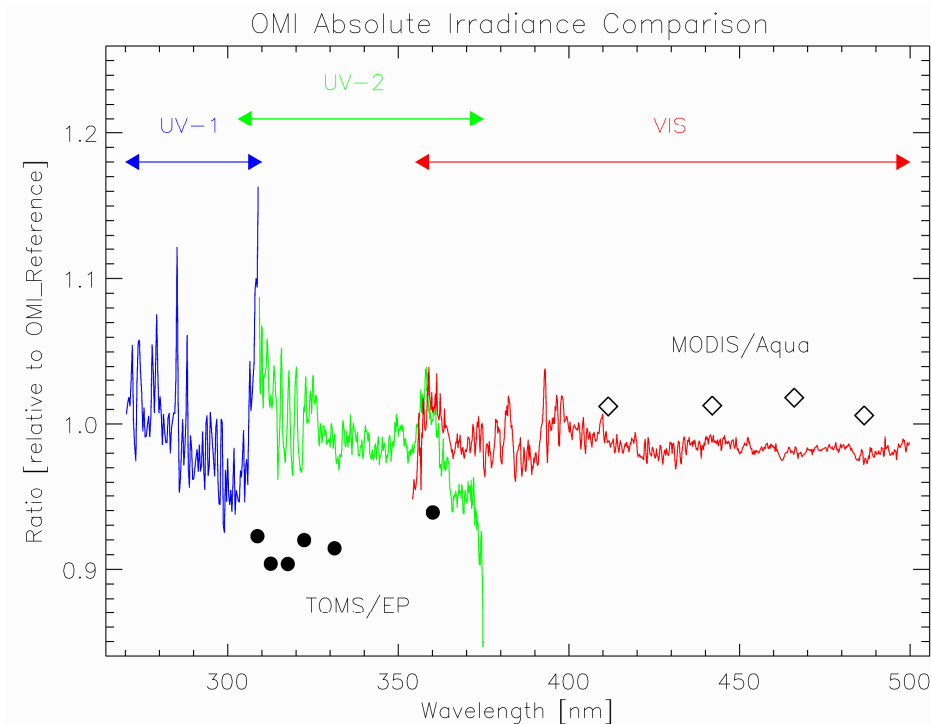


Figure 2. OMI measured solar irradiance (orbit 2465, 31 December 2004) comparison at the central (nadir) swath position, for the Volume diffuser, relative to the OMI solar reference spectrum. TOMS/EP (circles) and MODIS/Aqua solar irradiance (diamonds) comparisons are also shown.

3.1.2. Instrument calibration trends

The QVD diffuser's daily solar measurements provide data that permit high fidelity tracking of instrument calibration changes. The ground aluminum diffusers allow tracking of the primary diffuser's degradation, if any, that is common in many remote-sensing instruments. Figure 3 shows the normalized solar irradiances at nadir since regular on-orbit calibrations began. Gaps in the trend in mid-September and late November 2004 are due to early operations characterization measurements. The left panel illustrates the lack of any significant wavelength dependence as a function of time. The occasional 1-2% spikes seen in the surface are due to radiation hits on the focal plane causing temporary increases in signal at a given pixel. Plotting individual wavelengths in Figure 3b, small, 1% variations in the data become clear. Further analysis has shown that these wavelength independent variations are correlated in azimuth, and therefore, likely caused by small errors in the goniometry correction for this diffuser. Additional work is currently underway to more accurately characterize the diffuser goniometry. However, until an updated characterization is implemented, the QVD solar irradiance measurements can track instrument changes to only the 1% level.

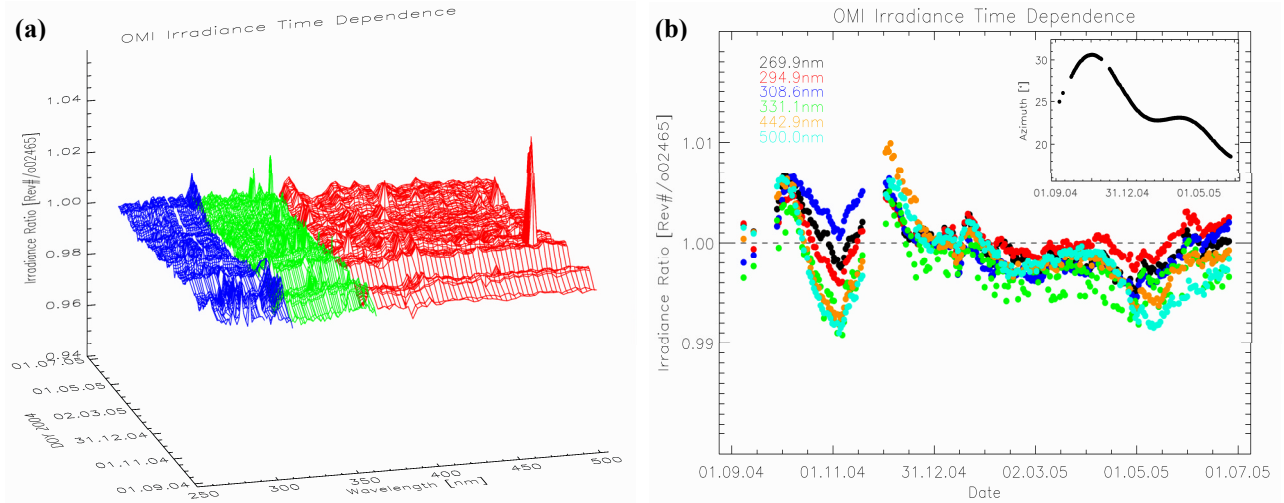


Figure 3. OMI measured solar irradiance trend at nadir swath position. The spectral and time dependent change surface in (a) shows each channel as a unique color. Specific wavelengths are shown in (b) to clearly show the minor time dependence in solar irradiance measurements. The inset plot in (b) shows the instrument solar azimuth angle as a function of time.

As mentioned in Section 2, OMI contains two additional ground aluminum diffusers, called Regular and Backup, whose purpose is to help distinguish between instrumental and diffuser changes in the QVD solar irradiance trends. The QVD differs from the Regular and Backup diffusers in that it has 6mm ground quartz with a ground aluminum backing, providing multiple scattering surfaces during solar observations⁷. Analysis has shown that the aluminum diffuser data exhibit large goniometric errors in swath, azimuth, and wavelength dependencies and are not suitable for trending purposes at this time. Figure 4 shows two example surfaces for the Regular and Backup diffuser irradiance trends (normalized to OMI solar reference irradiances) at nadir. In addition to the 5% time dependence, spectral structure can be seen in both surfaces at the lower VIS channel wavelengths that are on the same order of magnitude as those seen in the QVD data (see Figure 2). The UV channels also exhibit similar time dependencies.

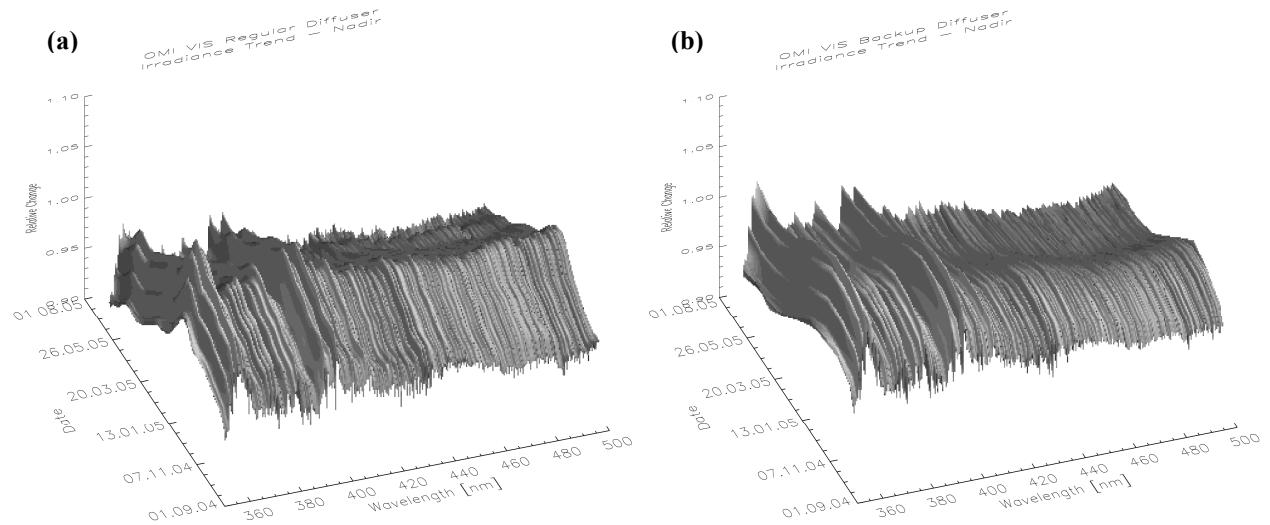


Figure 4. Regular (a) and Backup (b) diffuser solar irradiance time dependence at nadir for VIS wavelengths. OMI observed irradiances have been normalized to OMI solar reference irradiances.

3.2. Earth radiance comparisons

Solar irradiance measurements provide an important diagnostic tool in monitoring and characterizing instrument performance. However, in the case of OMI, the optical path used for solar measurements differs from that of Earth radiance measurements. The Earth view path includes the primary mirror, 003, but does not contain the solar aperture mesh, fold mirror, C03, and diffusers (see Figure 1). The primary and fold mirrors were designed to the same specifications so as to minimize any performance issues and the solar aperture mesh has been confirmed to be benign except signal attenuation. As shown in Section 3.1.3, the diffusers introduce their own swath dependent features that are not present in the radiance swath sensitivity. In order provide insight into the behavior of the radiance calibration and confirm that the measured solar irradiance trends are indicative of true instrument throughput changes, observations of ice and snow fields in Antarctica and Greenland were analyzed.

3.2.1. Ice field radiance trends

Observations of Antarctica and Greenland can be used to probe instrument radiometric performance due to the regenerative nature of the surfaces and relatively low atmospheric aerosol concentrations⁸. OMI observations of these regions from September to November 2004 were analyzed to confirm the instrument solar irradiance time dependence of instrument throughput. Figure 5 shows these normalized ice radiances at two wavelengths, 360nm in UV-2 and 460nm in VIS, over time with the normalized QVD solar irradiance over-plotted for the same time period. All data have been normalized to the average (ir)radiance from 7 to 14 November 2004 (orbits 1671 to 1787). In general, the time dependence of the radiances observed from Antarctica is flat, suggesting no instrument throughput changes occurred over this time period. The larger spread in the Greenland radiances at both wavelengths and the 460nm Antarctic radiances is likely due to seasonal effects in the respective hemispheres.

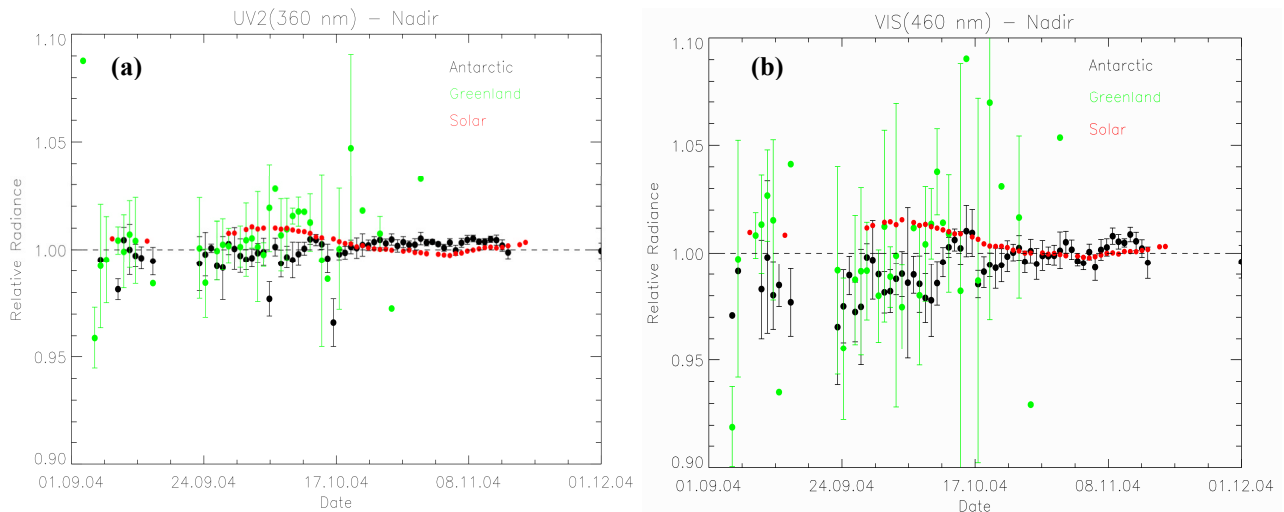


Figure 5. OMI ice radiances at nadir swath position. Solar irradiances and radiances over Antarctica (black) and Greenland (green) were normalized to their respective averages from 7 to 14 November 2004 (orbits 1671 to 1787). Error bars represent $\pm \sigma$ in the observed radiances.

3.2.2. Albedo swath angle dependence

The lack of large, uniform Earth radiance scenes makes on-orbit characterization of the instrument's swath angle dependence difficult. However, methods comparing measured Earth scenes to modeled radiances and analyzing radiance residuals from total column ozone retrievals were used to characterize this dependence. Top of the atmosphere (TOA) radiances based on a Gauss-Seidel atmospheric modeling code⁹ were calculated for all possible satellite viewing

conditions, sensor wavelengths, surface pressures, and total column ozone amounts. Minor absorption species, aerosols, clouds, and rotational Raman scattering were not included in the model calculations. Solar irradiance normalized differences were then computed between valid OMI Antarctic measurements and corresponding modeled calculations. Data were then binned by solar zenith angle (SZA) and instrument view angle, or swath position. Measurements made from 7 December 2004 to 4 January 2005 were analyzed resulting in a 3% swath angle dependence, as shown in Figure 6a. Only data within a SZA range from 62° to 67° were used. Lower SZA's limited the available satellite view angles (i.e. swath position) at these latitudes while the model becomes increasingly uncertain at larger SZA's.

Radiance residuals calculated from total column ozone retrievals were also investigated. OMI's implementation of a TOMS-like total column ozone retrieval, referred to as OMTO3, also provides the differences between the measured and calculated radiances for twelve specific wavelengths for diagnostics purposes¹⁰. These residuals were normalized to the measured solar irradiance and over-plotted as a function of swath position in Figure 6a. The swath dependence of the OMTO3 results shows a 3-4% change from nadir to the extreme view angles and agrees with the ice radiance results.

Small-scale structure differences between the two techniques could be the result of different solar irradiances used in the normalization. OMTO3 used solar data dated 28 March 2005, orbit 3725, while ice radiance differences were to data taken 27 December 2004, orbit 2402. Plotting the ratio of these two data sets and comparing the swath dependence at 331nm in Figure 6b shows a clear correlation in structure. Residual errors in the goniometric swath dependence are the likely cause of the changes in irradiance swath dependence.

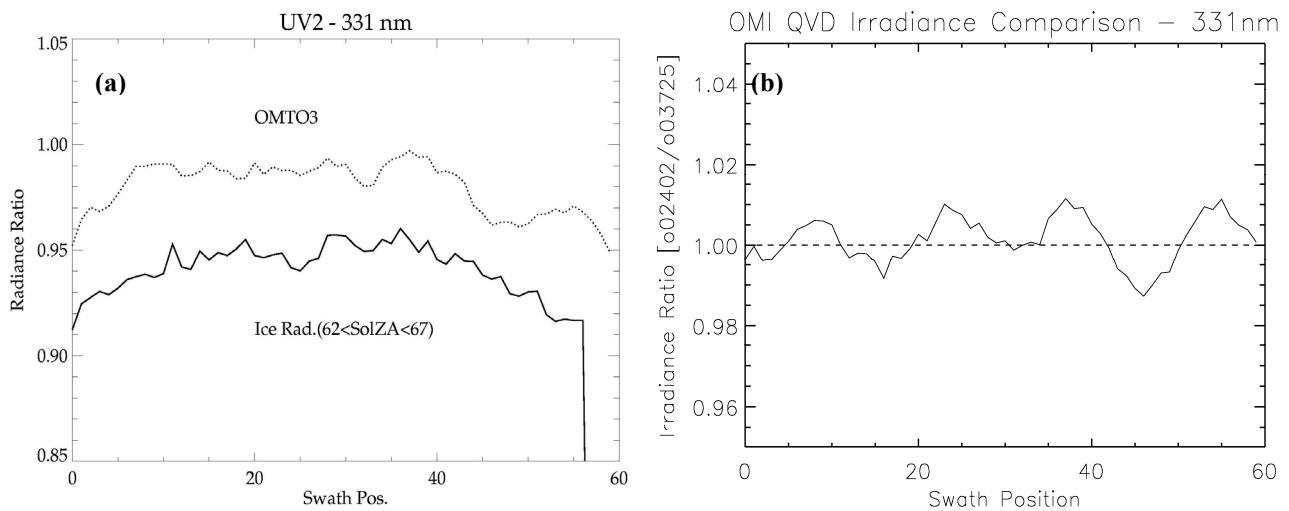


Figure 6. (a) OMI radiance swath dependence as determined by ice radiance comparisons to modeled calculations and total column ozone retrieval radiance residuals. (b) A comparison of the irradiance swath dependence between the different solar irradiance data used in this analysis shows a clear correlation with the structure in the OMTO3 data.

4. SUMMARY

Results from a variety of in-flight calibration analyses have been presented. Solar irradiance measurements have demonstrated that the instrument has not experienced any significant degradation to date in the observed wavelength ranges. This instrument stability has been confirmed through comparisons of Antarctic and Greenland ice radiances measured from September to November 2004. While only minor azimuthal goniometry errors exist at nadir for the QVD, further work is required to better characterize the azimuth and swath dependence for all diffusers in order to more accurately track instrument changes and be able to separate out diffuser degradation issues. Radiance residual analysis from the OMTO3 retrievals and ice radiances agree in the overall swath dependence of the OMI albedo calibration but are affected by issues related to the irradiance swath dependence. In general, the OMI instrument is performing well

during its first year of operation and characterization of instrument performance shall improve further based on future analyses.

ACKNOWLEDGEMENTS

The U.S. authors of this paper are supported under NASA contract NAS5-00220 and the Dutch authors are supported by the Netherlands Agency for Aerospace Programmes (NIVR).

REFERENCES

1. Jaross G., Krueger A., Cebula R.P., Seftor C., Hartmann U., Haring R., Burchfield D., "Calibration and postlaunch performance of the Meteor 3/TOMS instrument", *Journal of Geophysical Research*, 1995, **100**, no. D2, pp 2985-2995.
2. Huang L.K., Cebula R.P., Taylor S.L., Deland M.T., McPeters R.D., Stolarski R.S., "Determination of NOAA-11 SBUV/2 radiance sensitivity drift based on measurements of polar ice cap radiance", *International Journal of Remote Sensing*, 2003, **24**, no. 2, pp. 305-314.
3. Taylor S.L., Cebula R.P., Deland M.T., Huang L.K., Stolarski R.S., McPeters R.D., "Improved calibration of NOAA-9 and NOAA-11 SBUV/2 total ozone data using in-flight validation methods", *International Journal of Remote Sensing*, 2003, **24**, no. 2, pp. 315-328.
4. Woods T.N. *et al*, "Validation of the UARS solar ultraviolet irradiances: Comparisons with the ATLAS 1 and 2 measurements", *J. Geophys. Res.*, **101**, 9541-9569, 1996.
5. Tullier G., Floyd L., Woods T.N., Cebula R.P., Hilsenrath E., Herse M., Labs D., "Solar irradiance reference spectra for two solar active levels", *Advances in Space Research*, **34**, 256-261, 2004.
6. Jaross G., Wellemeyer C.G., Kelly T., Seftor C., Taylor S.L., Moy L., Labow G., "TOMS/Earth Probe Calibration: Low Orbit Period", Raytheon STX-3036-701-GJ-98-5, 1998.
7. Dobber M., "Ozone Monitoring Instrument calibration", submitted to *IEEE Trans. on Geosci. and Rem. Sens.*, 2005.
8. Jaross, G., Krueger A., Flittner D., "Multispectral calibration of remote sensing instruments over Antarctica", *Metrologia*, **35**, 625-629, 1998.
9. Herman, B., Caudill T., Flittner D., Thome K., Ben-David A., "A comparison of the Gauss-Seidel spherical polarized radiative transfer code with other radiative transfer codes", *Appl. Optics*, **34**, 4563-4572, 1995
10. <http://toms.gsfc.nasa.gov/omi/>